Equation of state of the unitary Fermi gas: An update on lattice calculations

Joaquín E. Drut, Timo A. Lähde, Gabriel Wlazłowski, and Piotr Magierski

Phys. Rev. A **85**, 051601 — Published 1 May 2012

DOI: 10.1103/PhysRevA.85.051601

The Equation of State of the Unitary Fermi Gas: An Update on Lattice Calculations

Joaquín E. Drut[1], Timo A. Lähde[2*], Gabriel Wlazłowski[3], and Piotr Magierski[3,4]
[1] *Theoretical Division, Los Alamos National Laboratory, Los Alamos, NM 87545–0001, USA*
[2] *Helsinki Institute of Physics, P.O. Box 64, FI-00014 University of Helsinki, Finland*
[3] *Faculty of Physics, Warsaw University of Technology, ulica Koszykowa 75, 00-662 Warsaw, Poland and*
[4] *Department of Physics, University of Washington, Seattle, Washington 98195-1560, USA*

The thermodynamic properties of the Unitary Fermi Gas (UFG) have recently been measured to unprecedented accuracy by Ku *et al.* at the MIT. In particular, these measurements provide an improved understanding of the regime below $T/\epsilon_F \simeq 0.20$, where a transition into a superfluid phase occurs. In light of this new development, we present an overview of state-of-the-art Auxiliary Field Quantum Monte Carlo (AFQMC) results for the UFG at finite temperature, comparing with the MIT data for the energy, chemical potential and density. These AFQMC results have been obtained using methods based on the Hybrid Monte Carlo (HMC) algorithm, which was first introduced within the context of Lattice QCD.

PACS numbers: 03.75.Ss 05.30.Fk 05.10.Ln

The Unitary Fermi Gas (UFG) is defined as a two-component many-fermion system in the limit of short interaction range r_0 and large s-wave scattering length a, such that $0 \leftarrow k_F r_0 \ll 1 \ll k_F a \to \infty$, with $k_F \equiv (3\pi^2 n)^{1/3}$ the Fermi momentum and n the particle number density (we choose units such that $\hbar = k_B = 1$). The UFG also saturates the unitarity bound on the quantum mechanical scattering cross section $\sigma_0(k) \leq 4\pi/k^2$, where k is the relative momentum of the colliding particles. The UFG features special properties that arise from the fact that it is characterized by a single length scale, given by the inter-particle distance $\sim k_F^{-1}$, independently of the details of the interaction. While the thermodynamic properties of the UFG are *universal* [1], the lack of a readily accessible dimensionless expansion parameter renders the UFG a challenging many-body problem. Since the proposal of the UFG as a model for dilute neutron matter by Bertsch [2] and its realization in ultracold atom experiments (see Ref. [3] for a review of the experimental situation), the UFG has received widespread attention, from atomic physics [4] to nuclear matter [5] and relativistic heavy-ion collisions [6].

On the experimental side, the presence of a superfluid phase in the UFG below $T/\epsilon_F \simeq 0.15$ was demonstrated directly a few years ago through the creation of an Abrikosov vortex lattice under rotation [7]. However, a direct thermodynamic signature of the transition was not unambiguously established until the recent high-precision measurement at the MIT of the Equation of State (EoS) of a homogeneous two-component UFG over a large temperature range [8]. These measurements were performed on trapped ^{6}Li atoms (using a Feshbach resonance to tune the system to the unitary limit), which enabled a detailed study of the compressibility, density and pressure of the UFG. In addition, greatly refined empirical results were obtained for the associated critical temperature $T_c/\epsilon_F = 0.167(15)$, as well as for the "Bertsch parameter" $\xi = 0.376(5)$, which characterizes the ground state of the UFG. As precision data is now available for the energy, chemical potential and density of the UFG in a wide temperature range, an opportunity presents itself to compare these measurements with calculations in various theoretical frameworks. Here, we focus on comparing the MIT data with the most recent Auxiliary Field Quantum Monte Carlo (AFQMC) results.

The Hamiltonian that captures the physics of the unitary limit can be written on a spatial lattice as

$$\hat{H} \equiv \sum_{\boldsymbol{k},\lambda=\uparrow,\downarrow} \frac{k^2}{2m}\, \hat{a}^\dagger_\lambda(\boldsymbol{k})\, \hat{a}_\lambda(\boldsymbol{k}) - g \sum_i \hat{n}_\uparrow(\boldsymbol{r}_i)\, \hat{n}_\downarrow(\boldsymbol{r}_i), \quad (1)$$

where λ denotes the spin projection, m the fermion mass (we also set $m = 1$), and g the coupling constant. The creation and annihilation operators satisfy fermionic anticommutation relations, and $\hat{n}_\lambda(\boldsymbol{r}_i) \equiv \hat{a}^\dagger_\lambda(\boldsymbol{r}_i)\, \hat{a}_\lambda(\boldsymbol{r}_i)$ denotes the number density operator at lattice position $\boldsymbol{r}_i$ for spin projection λ. The thermodynamic equilibrium properties are obtained from the partition function

$$\mathcal{Z} \equiv \mathrm{Tr}\, \exp[-\beta(\hat{H} - \mu\hat{N})], \quad (2)$$

where $\hat{N}$ is the total particle number operator, μ the chemical potential, and $\beta \equiv 1/T$ the inverse temperature.

To evaluate expectation values of observables numerically, we followed the path integral approach presented extensively in Ref. [9], with recent improvements described in Ref. [10]. The system is placed on a cubic spatial lattice of extent $L = N_x l$ with periodic boundary conditions. The lattice spacing l (henceforth set to unity) and extent L provide natural ultraviolet (UV) and infrared (IR) momentum cut-offs, given by $k_{\max} = \pi/l$ and $k_0 = 2\pi/L$, respectively. The imaginary-time evolution operator $\exp[-\beta(\hat{H} - \mu\hat{N})]$ is expanded using a

*Current address: Institut für Kernphysik (Theorie), Forschungszentrum Jülich, D-52425 Jülich, Germany

Trotter-Suzuki decomposition with temporal lattice spacing τ, and the interaction is represented by means of a Hubbard-Stratonovich (HS) transformation [11]. As we focus on the spin-symmetric case, the fermion sign problem is absent. The resulting path integral formulation is an exact representation of Eq. (2) up to finite-volume and discretization effects, which may be controlled by varying the spatial lattice volume $V \equiv N_x^3$ and density n. The thermodynamic and continuum limits are recovered as $V \to \infty$ and $n \to 0$, respectively. The latter requires great care, as too low densities may introduce shell effects. As our lattice formulation is very similar to Ref. [9], we shall restrict ourselves to describing three modifications which significantly improve the results.

First, the bare lattice coupling constant g corresponding to the unitary regime is determined by means of Lüscher's formula [12] as in Ref. [13]. This procedure yields $g \simeq 5.14$ in the unitary limit. Our lattice Hamiltonian contains g as the sole parameter characterizing the interaction. Finite-range effects are induced by the presence of the UV cutoff of the lattice. In order to minimize such discretization effects, the dilute limit should be approached as closely as possible. Recent theoretical developments [14–16] have explored the use of improved transfer matrices and operators, with multiple parameters tuned to unitarity. The implementation of such methods is an objective of future AFQMC calculations.

Second, we use a compact, continuous HS transformation referred to as "Type 4" in Ref. [17], which found it superior with respect to acceptance rate, decorrelation and signal-to-noise properties than the more conventional unbounded and discrete HS transformations [18].

Third, we update σ using Hybrid Monte Carlo (HMC), which combines Molecular Dynamics (MD) evolution of σ with a Metropolis accept/reject step [19]. The result is the Determinantal Hybrid Monte Carlo (DHMC) algorithm, introduced in Ref. [10]. In DHMC, global MD updates of σ take place via introduction of a momentum field π conjugate to σ, such that the dynamics is given by the Hamiltonian

$$\mathcal{H} \equiv \sum_i \frac{\pi_i^2}{2} - \log\det\left[(\mathbb{1} + \mathcal{U}[\sigma])^2\right], \qquad (3)$$

where $\mathcal{U}[\sigma]$ encodes the dynamics of the fermion degrees of freedom (for more details on $\mathcal{U}$, see *e.g.* Ref. [9]). The DHMC algorithm produces greatly enhanced decorrelation between successive MC samples for all temperatures and lattice sizes, and removes the necessity to spend an increasing number of decorrelation steps at larger V (note that the computational cost of a full sweep of the lattice scales as $\sim V$ in a local algorithm such as DMC). This is replaced by a fixed number of operations, typically of $\mathcal{O}(10^2)$, required to produce one MD "trajectory", independently of V.

The DHMC algorithm allows for an extension of the AFQMC analysis beyond the capabilities of DMC, which is currently limited to $N_x \simeq 10$ in the spatial lattice extent, $n \simeq 0.1$ in particle number density, and $N \simeq 100$ in the particle number. The improved scaling of the CPU time has allowed us to study lattices up to $N_x = 16$, while simultaneously maintaining a relatively large number of particles, $N \simeq 45, 75, 110$ and 160 for $N_x = 10, 12, 14$ and 16, respectively, which corresponds to densities in the range $n \simeq 0.040 - 0.045$. The $N_x = 8$ data (which are not identical to Ref. [9]), correspond to $N \simeq 35$ and $n \simeq 0.070$, which was not reduced further in order to avoid shell effects. We generated $\simeq 200$ uncorrelated snapshots of σ for each value of T/ϵ_F, which yields a statistical uncertainly of $\simeq 1\%$ for the observables. Expressions for the AFQMC computation of the latter were obtained by differentiating $\mathcal{Z}$ with respect to β and μ as conventional in thermodynamics, with the exception that $\mathcal{Z}$ is replaced by its discretized form in terms of the HS field.

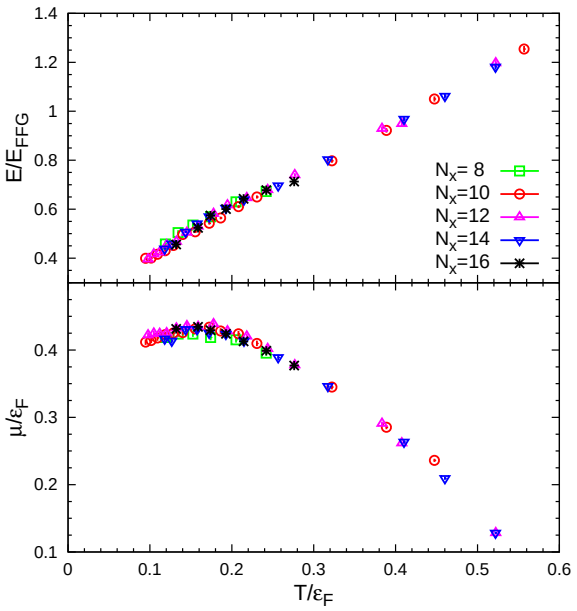

FIG. 1: (Color online) AFQMC results for the total energy E in units of the energy of a free Fermi gas (upper panel) and the chemical potential μ in units of the Fermi energy (lower panel) as a function of T/ϵ_F. Results are shown for $N_x = 8$ (green squares), $N_x = 10$ (red circles), $N_x = 12$ (purple triangles), $N_x = 14$ (blue inverted triangles), and $N_x = 16$ (black asterisks), where $V \equiv N_x^3$ is the (spatial) lattice volume.

In Fig. 1, we present AFQMC results (for various lattice sizes) for the total energy E in units of the energy of a free Fermi gas $E_{\rm FG} = 3/5 N \epsilon_F$, and for the chemical potential μ in units of ϵ_F as a function of T/ϵ_F. Before comparison with the MIT data [8], we performed an extrapolation to the infinite volume limit $N_x \to \infty$. This required interpolation of the data series for each value of N_x, as the physical temperature T/ϵ_F is not known beforehand. Apart from this minor complication, the extrapolation to infinite volume is greatly facilitated by the lack of a systematic variation in the results with the lattice volume above $N_x \simeq 10$. Since we have not performed an extrapolation to the continuum limit (which requires

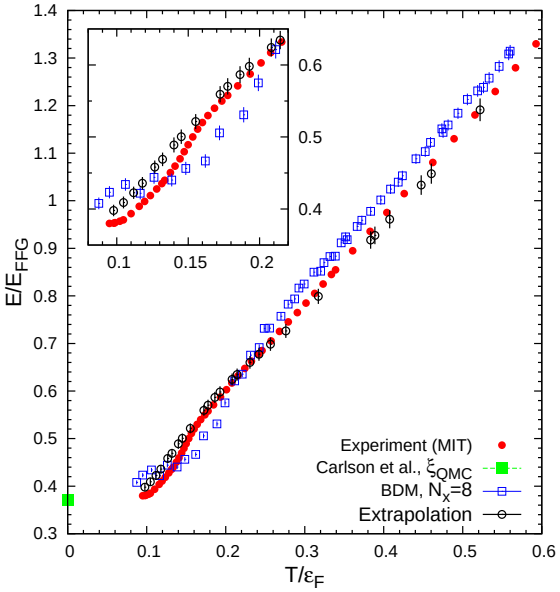

FIG. 2: (Color online) Energy $E/E_{\rm FG}$ (red dots), as obtained by Ku *et al.* [8]. Our AFQMC results extrapolated to infinite volume are shown by open (black) circles. The results for $N_x = 8$ (open blue squares) were obtained with the DMC algorithm in Ref. [9]. The green square shows the QMC result of Ref. [20] for ξ at $T = 0$. Inset: Vicinity of the superfluid phase transition at $T_c/\epsilon_F \simeq 0.15$.

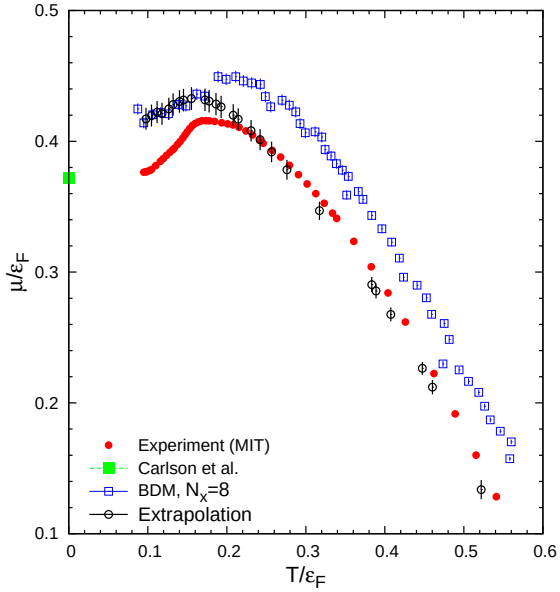

FIG. 3: (Color online) Chemical potential μ in units of ϵ_F as measured by Ku *et al.* [8]. The notation for the AFQMC results is identical to Fig. 2. The (green) square shows the result of Ref. [20] assuming $\mu/\epsilon_F(T = 0) = \xi$.

$n \to 0$), our results may be affected to some degree by systematic errors due to the effective range $r_{\rm eff}$. Our results currently reach $k_F r_{\rm eff} \simeq 0.3$ which is non-negligible and may produce significant deviations, in particular at low T/ϵ_F as shown by Carlson *et al.* in Ref. [20].

In Fig. 2, we compare our AFQMC results (extrapolated to infinite volume) with the measured energy E of the homogeneous UFG. The overall agreement is satisfactory throughout the range of temperatures studied. At low T/ϵ_F, AFQMC slightly overpredicts the experimental data. Our new results show a noticeable improvement over the results of Ref. [9] with $N_x = 8$, likely due to decreased finite volume and effective range effects. In contrast to the case of $E/E_{\rm FG}$, our results for μ/ϵ_F in Fig. 3 deviate noticeably from experiment at low T/ϵ_F, where $\mu/\epsilon_F \simeq 0.38$ at $T/\epsilon_F \simeq 0.1$. AFQMC overpredicts this by $\simeq 5\%$, which clearly exceeds the statistical uncertainty. However, the larger lattices used here represent a dramatic improvement over Ref. [9], in particular above $T_c/\epsilon_F \simeq 0.15$. Nevertheless, the discrepancy below T_c/ϵ_F cannot be accounted for at present. In Fig. 4, we show the particle number density relative to the temperature-dependent density of the non-interacting Fermi gas. Again, a discrepancy at low T/ϵ_F is found, which is analogous to that observed for μ/ϵ_F.

While the agreement between our AFQMC calculation and the data of Ref. [8] is satisfactory in general, notable discrepancies persist. We have achieved a significant reduction of the density from $n \simeq 0.1$ to $n \simeq 0.04$, with a concomitant decrease in discretization (finite-range) effects. Nevertheless, since finite-range effects scale as $\sim n^{1/3}$, this still only implies an effective reduction from $n^{1/3} \simeq 0.46$ to $\simeq 0.34$. The possibility that the discrepancies between our AFQMC data and experiment are due to residual finite-range effects can therefore not be ruled out at present.

As the region where the discrepancies are largest appears to be at very low T/ϵ_F (at least for $E/E_{\rm FG}$ and μ/ϵ_F), the task of performing calculations at significantly lower values of $n^{1/3}$ for such temperatures is extremely demanding, indeed largely beyond the capabilities of extant algorithms. In this situation, accounting for the finite-range effects by improving the transfer matrix (as in Refs. [14, 15]) provides a systematic way to remove the finite-range effects from both the action and the observables at a given density, without modifying the temperature scale of the calculation. Preliminary results have appeared in Ref. [16]. Another source of error under investigation is the Trotter-Suzuki step τ. This was found to be a small effect for the Tan contact in Ref. [10], as well as for the energy in Ref. [15].

In spite of these shortcomings, the introduction of HMC into the AFQMC study of the UFG has largely solved the issue of sufficiently large spatial lattice dimension N_x and particle number N, which in turn has allowed calculations with a large particle number at lower densities. DHMC studies for $N_x > 16$ are in progress. These improvements will also apply to calculations away from the unitary limit. Finally, we would like to stress that the AFQMC method is entirely *ab initio* - once the coupling g is fixed by solving the two-body problem, no tuning with respect to experiment is required. While a more

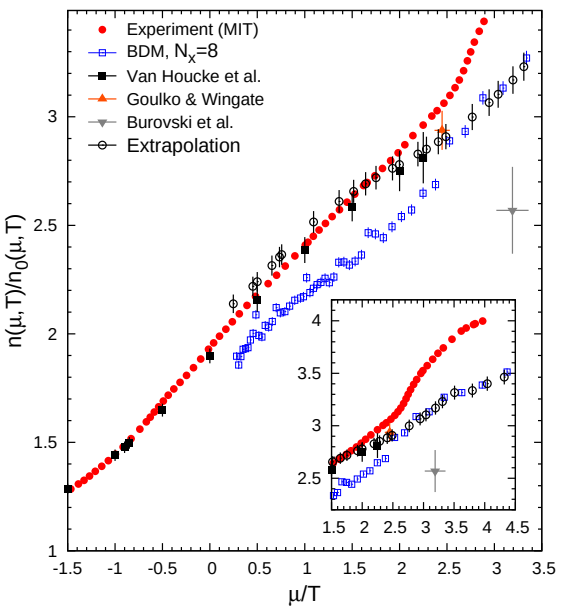

FIG. 4: (Color online) Density $n(\mu, T)$ of the UFG (red circles) as obtained by Ku *et al.* [8], normalized to the density $n_0(\mu, T)$ of a non-interacting Fermi gas. The notation for the AFQMC results is identical to Fig. 2. The Diagrammatic MC results of Refs. [21, 22] (filled up and down triangles) and the BDMC results of Ref. [23] are shown as well (filled squares). Inset: Vicinity of the superfluid phase transition at $T_c/\epsilon_F \simeq 0.15$.

sophisticated analysis of the systematic errors cannot be provided at this point in time, the fact that theory and experiment agree reasonably well for both $E/E_{\rm FG}$ and μ/ϵ_F over a wide range of temperatures is both remarkable and encouraging.

We thank M. Zwierlein for making the MIT data available, and F. Werner for providing us with the BDMC results. We are also indebted to A. Bulgac for instructive discussions and a careful reading of the manuscript. We acknowledge support under U.S. DOE Grant DE-FC02-07ER41457, and contract N N202 128439 of the Polish Ministry of Science. This study was supported, in part, by the Vilho, Yrjö, and Kalle Väisälä Foundation of the Finnish Academy of Science and Letters, and by the Magnus Ehrnrooth, the Waldemar von Frenckell and the Nils-Erik and Ruth Stenbäck Foundations of the Finnish Society of Sciences and Letters. One of the authors (G.W.) acknowledges the Polish Ministry of Science for the support within the program "Mobility Plus - I edition" under contract No. 628/MOB/2011/0. Part of the computer time for this study was provided by the Interdisciplinary Centre for Mathematical and Computational Modeling (ICM) at the University of Warsaw.

[1] H. Heiselberg, Phys. Rev. A **63**, 043606 (2001); T.-L. Ho, Phys. Rev. Lett. **92**, 090402 (2004).
[2] "The Many-Body Challenge Problem", formulated by G. F. Bertsch (1999), see *e.g. Series on Advances in Quantum Many-Body Theory - Vol. 3*, R. F. Bishop, K. A. Gernoth, N. R. Walet, Y. Xian (Eds.) (World Scientific, Singapore, 2000).
[3] *Ultracold Fermi Gases*, Proceedings of the International School of Physics "Enrico Fermi", Course CLXIV, Varenna, June 20 – 30, 2006, M. Inguscio, W. Ketterle, C. Salomon (Eds.) (IOS Press, Amsterdam, 2008).
[4] S. Giorgini, L. P. Pitaevskii, S. Stringari, Rev. Mod. Phys. **80** (2008) 1215; I. Bloch, J. Dalibard, W. Zwerger, *ibid.* **80** (2008) 885.
[5] C. J. Pethick, D. G. Ravenhall, Ann. Rev. Nucl. Part. Science **45**, 429 (1995); J. Carlson *et al.*, Phys. Rev. C **68**, 025802 (2003); C. J. Horowitz, A. Schwenk, Phys. Lett. B **638** 153 (2006). A. Gezerlis, J. Carlson, Phys. Rev. C **77**, 032801(R) (2008).
[6] T. Schäfer, Physics **2**, 88 (2009); T. Schäfer, D. Teaney, Rept. Prog. Phys. **72**, 126001 (2009).
[7] M. W. Zwierlein *et al.* Nature **435**, 1047 (2005).
[8] M. J. H. Ku, A. T. Sommer, L. W. Cheuk, M. W. Zwierlein, Science **335**, 563 (2012).
[9] A. Bulgac, J. E. Drut, P. Magierski, Phys. Rev. Lett. **96**, 090404 (2006); Phys. Rev. A **78**, 023625 (2008); A. Bulgac, M. M. Forbes, P. Magierski, in *BCS-BEC Crossover and the Unitary Fermi Gas* (Chap. 9), W. Zwerger (Ed.) (Springer, Berlin, 2011), *to be published*.
[10] J. E. Drut, T. A. Lähde, T. Ten, Phys. Rev. Lett. **106**, 205302 (2011).
[11] R. L. Stratonovich, Sov. Phys. Dokl. **2**, 416 (1958); J. Hubbard, Phys. Rev. Lett. **3**, 77 (1959).
[12] M. Lüscher, Commun. Math. Phys. **105**, 153 (1986).
[13] D. Lee, T. Schäfer, Phys. Rev. C **73**, 015201 (2006); Phys. Rev. C **73**, 015202 (2006).
[14] M. G. Endres, D. B. Kaplan, J.-W. Lee, A. N. Nicholson, arXiv:1106.5725; arXiv:1106.0073; PoS **LAT2010**, 182 (2010); J.-W. Lee, M. G. Endres, D. B. Kaplan, A. N. Nicholson, arXiv:1011.3026; PoS **LAT2010**, 197 (2010); A. N. Nicholson, M. G. Endres, D. B. Kaplan, J.-W. Lee, arXiv:1011.2804; PoS **LAT2010**, 206 (2010).
[15] M. G. Endres, D. B. Kaplan, J.-W. Lee, A. N. Nicholson, arXiv:1203.3169.
[16] J. E. Drut, arXiv:1203.2565.
[17] D. Lee, Phys. Rev. C **78**, 024001 (2008); Prog. Part. Nucl. Phys. **63**, 117 (2009).
[18] J. E. Hirsch, Phys. Rev. B **28**, 4059(R) (1983).
[19] S. Duane *et al.*, Phys. Lett. B **195**, 216 (1987); S. A. Gottlieb *et al.*, Phys. Rev. D **35**, 2531 (1987).
[20] J. Carlson *et al.*, Phys. Rev. A **84**, 061602(R) (2011)
[21] E. Burovski, N. Prokof'ev, B. Svistunov, M. Troyer, Phys. Rev. Lett. **96**, 160402 (2006).
[22] O. Goulko, M. Wingate, Phys. Rev. A **82**, 053621 (2010).
[23] K. Van Houcke *et al.*, arXiv:1110.3747.